# Regular periodic intersubband photocurrent peaks in a multiple double-well structure

H. C. Liu, Jianmeng Li,* M. Buchanan, Z. R. Wasilewski, and J. G. Simmons*
*Institute for Microstructural Sciences, National Research Council, Ottawa, Ontario, Canada K1A 0R6*
(Received 17 February 1993)

Strikingly regular periodic intersubband photocurrent peaks are observed in a multiple-quantum-well (MQW) structure in which the periodic unit is a coupled double well. A phenomenological model is proposed and is used to explain the observed results. The complexity of the transport problem for a MQW structure in the physical regime studied here is discussed.

Special electronic transport properties in superlattices and quantum wells give rise to interesting physical phenomena and useful devices. There are several different regimes for superlattice (SL) and multiple-quantum-well (MQW) carrier transport. When a SL or a MQW is not doped and the electrostatic effect due to the charged carriers can be neglected, the problem involves solving only the Schrödinger equation. Within this regime, many novel features have been reported.[1–4] When the SL or MQW is doped or the charge buildup is nonnegligible, however, one must consider simultaneously both the Schrödinger and Poisson equations. In this case, the charge redistribution within the SL or MQW can give rise to distinct features in device characteristics.[5–8] Studies of carrier transport in SL and MQW structures also have practical implications, and may result in new microwave oscillators[9] and infrared emitters,[10,11] and also may lead to further improvements in the design of intersubband infrared detectors.[12,13] A good example is the study of resonant tunneling which has produced high-speed double-barrier diodes.[14] In this paper, we report on our experimental study of intersubband photocurrent in a MQW structure with a coupled double-well period. The same coupled-well MQW structure has been investigated for making infrared modulators.[15,16] MQW structures with double-well period have also been used to study coherent versus sequential resonant-tunneling mechanisms.[17]

Our sample was grown by molecular-beam epitaxy. The period of the 40 repeat MQW structure consists of a wide (7.6 nm) and a narrow (4.0 nm) GaAs well separated by a thin (3.0 nm) $Al_{0.42}Ga_{0.58}As$ barrier. The center 4.0 nm of the wide well was doped with Si to $2.0 \times 10^{18}$ cm$^{-3}$ giving rise to a two-dimensional electron gas with a Fermi energy of $E_F = 0.028$ eV. The separation between adjacent periods is a 17.0-nm $Al_{0.42}Ga_{0.58}As$ barrier. The top (310 nm) and the bottom (620 nm) GaAs contact layers were doped with Si to $2.0 \times 10^{18}$ cm$^{-3}$. The wide quantum well contains two confined states at $E_0 = 0.05$ eV and $E_1 = 0.19$ eV, and the narrow quantum well contains one confined state at $E_0' = 0.11$ eV, and a second quasiconfined state $E_1' = 0.34$ eV in resonance with the top of the barrier.

The basic idea is shown schematically in Fig. 1. We consider only the voltage polarity (defined as positive) appropriate to the potential profile shown in the figure. Under low applied bias ($< 1.5$ V), the observed current is due to interperiod tunneling between the $E_0$ levels of adjacent periods. As the electric field is increased, $E_0'$ is lowered with respect to the Fermi level associated with $E_0$ in the same period, and electron transfer into to $E_0'$ takes place.[16] The current between about 1.5 and 3 V bias is due to interperiod tunneling of the electrons in $E_0$ and $E_0'$ of one period to the same states in the next period. As the electric field is further increased, this interperiod tunneling can no longer occur throughout the entire MQW structure, since the confined states cannot be aligned energetically, and one of the periods breaks into a high-field domain where tunneling is accommodated by tunneling nearly into but slightly below $E_1$ of the next period to maintain current continuity.[7,8] Further increases in bias voltages lead to a sequential expansion of the high-field domain by one period at a time. This high–low-field domain formation is well known and has been reported in several publications.[5–8] The uniqueness of the present structure comes from the arrangement of the confined states. Because $E_1$ is relatively deep in the wide well, extremely regular sequential resonant-tunneling peaks can be observed as shown in Fig. 2. Furthermore, because $E_1'$ in the narrow well is in resonance with the top of the barrier, a large intersubband photocurrent associated with the $E_0'$ to $E_1'$ transition can be observed when electrons are transferred into $E_0'$ from $E_0$.[16] In contrast, conventional MQW single-well period intersubband detector structures with two bound states would have to trade off between the regularity of sequential resonant-tunneling peaks and the photocurrent response. Using our MQW

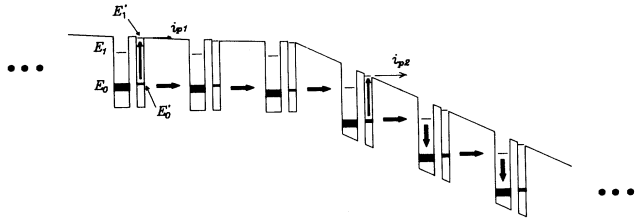


FIG. 1. Conduction-band-edge profile under an applied voltage. The left-hand part shows the ground-state interperiod tunneling process in the low-field domain, and the right-hand part is for the high-field domain where the current path is through sequential ground-to-excited-state interperiod tunneling. Intersubband photocurrents in the low- and the high-field domains are $i_{p1}$ and $i_{p2}$, respectively.

structure, we can therefore study simultaneously both sequential resonant-tunneling and intersubband photocurrent.

Mesa diode devices were made by standard wet chemical etching and contacts were formed by alloyed NiGeAu. A 45° edge facet was polished near the mesa for optical coupling to the device.[13] A 140 × 290-$\mu m^2$ device was mounted in a liquid-nitrogen-cooled cold-finger cryostat, and the actual device temperature was about 81 K. A series load resistor, an optical chopper, and a lock-in amplifier were used to measure photocurrent. The infrared source was a 1000 K blackbody, with the excitation wavelength selected by a variable filter monochromator. The measured photocurrent is defined as the measured voltage change on the lock-in amplifier across the load resistor divided by the load resistance. The measured photocurrent is independent of chopping frequency up to about 3 kHz, and then starts to deviate slightly due to the circuit $RC$ limit.

Our experimental results are shown in Figs. 2 and 3. The wavelength of the infrared light is 6.2 $\mu$m which corresponds to the peak of the $E_0'$ to $E_1'$ intersubband transition.[16] The transition from $E_0$ to $E_1$ does *not* produce a photocurrent because photoexcited electrons cannot escape from $E_1$.[16] We observe distinct differences in scans with increasing and decreasing voltages both for the device current-voltage ($I$-$V$) and the photocurrent-voltage ($I_p$-$V$) characteristics. To our knowledge, this is the first time that a hysteresis has been reported in the $I$-$V$ curves associated with sequential MQW resonant tunneling, and also the first time that regular periodic photocurrent peaks have been observed experimentally. To confirm that the observed device current is due to a pure tunneling process, $I$-$V$ curves were also measured at a device temperature of 4.2 K where thermionic emission from the wells is completely negligible, and *identical* results as shown in Fig. 2 were obtained.

To quantitatively model the observed results including both the transport and the charge redistribution

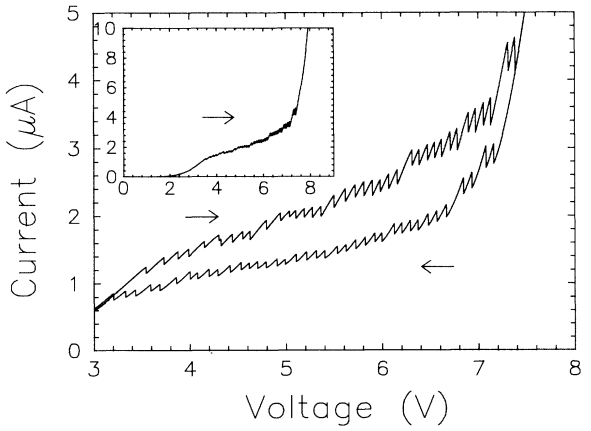


FIG. 2. Device current-voltage curves at 81 K. The voltage scan direction is indicated by the arrows. The inset shows a full increasing voltage scan.

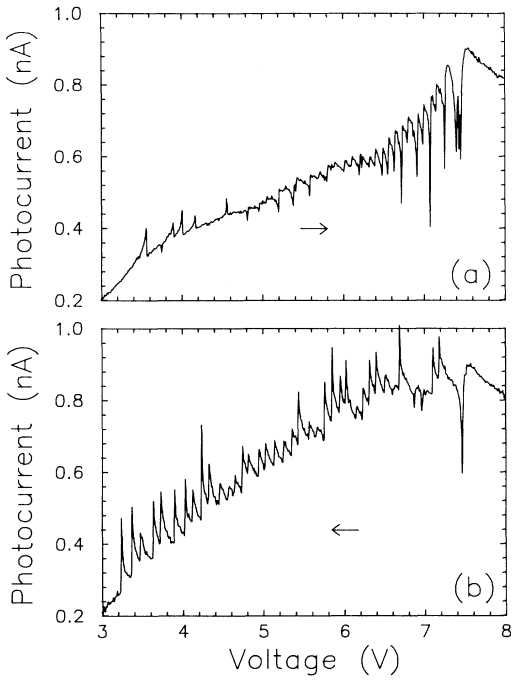


FIG. 3. Measured intersubband photocurrent versus voltage at 81 K. (a) and (b) are for increasing and decreasing voltage scans, respectively.

self-consistently is a very complicated problem, and indeed has not been done even for the single-well-period MQW's.[5–8] The main difficulty, in our opinion, arises from the absolute need for self-consistency between transport and electrostatics, or between the Schrödinger and Poisson equations. This is seen easily by considering the joining point of the low- and the high-field domains in a MQW structure. This joining point has the property that the electric field is low to its left and high to its right (or vice versa). This means that there must be a large charge accumulation (or depletion) at that point in order to cause this rapid change in field. Furthermore, these extra electrons (or absence of electrons) would result in an extra current flow towards the low-field region to the left (or the lack of a current flow to the right). There must therefore be a redistribution of electrons in periods adjacent to the joining point in order to maintain current continuity. The reality is therefore far more complicated than simply picturing two domains with low and high constant fields. Sorting out this self-consistent redistribution can be a computationally intractable problem.

To understand our experimental results qualitatively, we use a phenomenological model (shown in Fig. 4), in which the low- and the high-field domains are modeled as two dynamic resistances in series ($r_1$ and $r_2$), and the photocurrents in the low- and the high-field domains are $i_{p1}$ and $i_{p2}$, respectively. The interperiod tunneling probability is also shown schematically, with the low-field ground state resonance ($0 \rightarrow 0$) and the high-field ground-to-excited state resonance ($0 \rightarrow 1$) indicated. The difference in forward and reverse voltage scan $I$-$V$

curves (labeled by $I$-$V_{\rightarrow}$ and $I$-$V_{\leftarrow}$) can be qualitatively understood with the help of the interperiod tunneling probability versus electric field, schematically shown in Fig. 4. When the applied voltage is increased, the low-field region reaches a critical point at a field $F_{c1}$ where a switchover of one period into the high-field domain occurs, and the $I$-$V_{\rightarrow}$ curve then follows the upper hatched region. Similarly, when the applied voltage is decreased, the high-field region reaches a critical point at a field $F_{c2}$, and the $I$-$V_{\leftarrow}$ curve then follows the lower hatched region. The two hatched regions are not identical because when the switchover of a period from low to high (or high to low) field occurs, the field in the low- (or high-) field domain needs to change just enough to balance the amount of high (or low) field for one period.

Using the same model and incorporating the photocurrents, we can interpret the different behaviors in the observed forward and reverse voltage photocurrent versus voltage scans. The measured photocurrent, defined as the measured voltage change across the load resistor due to infrared illumination divided by the series resistance, is found easily using the equivalent circuit shown in Fig. 4:

$$I_p = \frac{i_{p1}r_1 + i_{p2}r_2}{R_s + r_1 + r_2}, \tag{1}$$

where $R_s$ is the resistance of the load. We assume that the photocurrents generated in the low- and high-field domains, $i_{p1}$ and $i_{p2}$, are slowly varying functions of the bias voltage. We also expect $i_{p1}$ to be much less than $i_{p2}$ (if the high-field domain is not too small), because the number of electrons in $E_0'$ (which have been transferred from $E_0$) is much less for the low-field domain than that for the high-field domain. For $I_p$-$V_{\leftarrow}$, the field in the high-field domain reaches the point $F_{c2}$ before a switchover occurs. At $F_{c2}$, the dynamic resistance $r_2$ becomes very large, and a maximum in the observed photocurrent $I_p$ occurs according to Eq. (1). This explains the strikingly regular periodic peak structures shown in Fig. 3(b). The explanation of the $I_p$-$V_{\leftarrow}$ behavior involves only the rapid increase of $r_2 \rightarrow \infty$ at $F_{c2}$, while the other parameters ($i_{p1}$, $i_{p2}$, and $r_1$) remain nearly constant. The situation is slightly more complicated for $I_p$-$V_{\rightarrow}$. When the voltage is increased from zero, but is still small, there is *no* high-field domain, and both $i_{p2}$ and $r_2$ are zero; hence when $r_1 \rightarrow \infty$ at $F_{c1}$, $I_p$ displays a maximum at $F_{c1}$. After the first switchover, this behavior may still dominate for the next few switchovers because although $i_{p2}$ is increasing, it is still small by comparison to $i_{p1}$. However, once $i_{p2}$ becomes much larger than $i_{p1}$, the contribution from $i_{p1}$ in Eq. (1) can be neglected, and the effect of $r_1 \rightarrow \infty$ at $F_{c1}$ is to produce periodic minima in $I_p$ as seen in Fig. 3(a) for voltages above about 6 V.

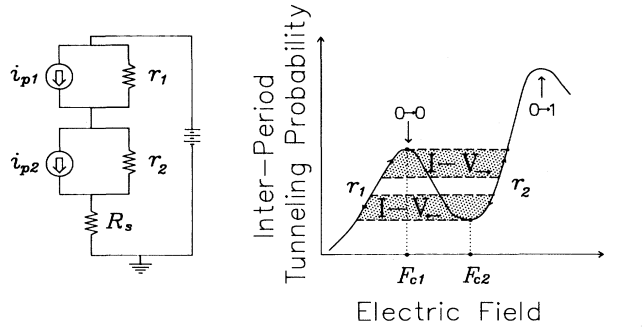


FIG. 4. Left-hand side: the model equivalent circuit; right-hand side: the schematic interperiod tunneling probability.

Additional measurements (not shown) of capacitance-voltage ($C$-$V$) curves were made at 77 K, and regular peaks in the $C$-$V$ curves were observed, which also can be modeled using an equivalent circuit of serially connected pairs of parallel resistors and capacitors.

To conclude, there is clearly a need for more studies in order to understand more fully the transport properties in SL and MQW structures in the regime where both high- and low-field domains exist. The solution to the complicated domain formation and evolution problem must be sought using a self-consistent approach which includes both tunneling current and electrostatics. A self-consistent microscopic model may also provide guidelines for designing new microwave and infrared devices.

The authors thank R. Borris, P. Chow-Chong, Zhaohui Li, P. Marshall, and J. Stapledon for sample preparation; J. Thompson for technical support, and Dr. D. Landheer for assistance in $C$-$V$ measurements. The authors have also benefited from many discussions with Dr. G. C. Aers and Dr. A. G. Steele.

* Also at Centre for Electrophotonic Materials and Devices, McMaster University, Hamilton, Ontario, Canada L8S 4M1.

[1] F. Capasso, K. Mohammed, and A. Y. Cho, Appl. Phys. Lett. **48**, 478 (1986).
[2] A. Sibille, J. F. Palmier, H. Wang, and F. Mollot, Phys. Rev. Lett. **64**, 52 (1990).
[3] F. Beltram, F. Capasso, D. L. Sivco, A. L. Hutchinson, S.-N. G. Chu, and A. Y. Cho, Phys. Rev. Lett. **64**, 3167 (1990).
[4] X. L. Lei, H. J. M. Horing, and H. L. Cui, Phys. Rev. Lett. **66**, 3277 (1991).
[5] L. Esaki and L. L. Chang, Phys. Rev. Lett. **33**, 495 (1974).
[6] K. K. Choi, B. F. Levine, R. J. Malik, J. Walker, and C. G. Bethea, Phys. Rev. B **35**, 4172 (1987).
[7] H. T. Grahn, R. J. Haug, W. Müller, and K. Ploog, Phys. Rev. Lett. **67**, 1618 (1991).
[8] P. Helgesen, T. G. Finstad, and K. Johannessen, Appl. Phys. Lett. **69**, 2689 (1991).
[9] L. Esaki and R. Tsu, IBM J. Res. Dev. **14**, 61 (1970).
[10] R. F. Kazarinov and R. A. Suris, Fiz. Tekh. Poluprovodn. **6**, 148 (1972) [Sov. Phys. Semicond. **6**, 120 (1972)].

[11] H. C. Liu, J. Appl. Phys. **63**, 2856 (1988); **69**, 2749(E) (1991).
[12] *Intersubband Transitions in Quantum Wells*, edited by E. Rosencher, B. Vinter, and B. F. Levine (Plenum, New York, 1992).
[13] B. F. Levine, Appl. Phys. Rev. (to be published).
[14] T. C. L. G. Sollner, E. R. Brown, W. D. Goodhue, and H. Q. Le, in *Physics of Quantum Electron Devices*, edited by F. Capasso, Springer Series in Electronics and Photonics Vol. 28 (Springer-Verlag, Berlin, 1990), Chap. 6.
[15] M. Paton and H. C. Liu, Supperlat. Microstruct. **4**, 737 (1988).
[16] H. C. Liu, A. G. Steele, M. Buchanan, and Z. R. Wasilewski, J. Appl. Phys. **70**, 7560 (1991).
[17] K. K. Choi, B. F. Levine, C. G. Bethea, J. Walker, and R. J. Malik, Phys. Rev. Lett. **59**, 2459 (1987).